Sedimentary Geology, 64 (1989) 79–90
Elsevier Science Publishers B.V., Amsterdam – Printed in The Netherlands

Pyrite mineralization in microbial mats from the mid-Proterozoic Newland Formation, Belt Supergroup, Montana, U.S.A.

JÜRGEN SCHIEBER

Department of Geology, University of Texas at Arlington, Arlington, TX 76019 (U.S.A.)

Received August 15, 1988; revised version accepted March 2, 1989

Abstract

Schieber, J., 1989. Pyrite mineralization in microbial mats from the mid-Proterozoic Newland Formation, Belt Supergroup, Montana, U.S.A.. Sediment. Geol., 64: 79–90.

The Mid-Proterozoic Newland Formation, a shale-dominated unit of the Belt Supergroup, was deposited in an eastern extension of the Belt basin, the Helena embayment. A variety of different shale facies types can be distinguished. Of particular interest for this study is a shale facies that has been interpreted to be the result of microbial mat growth (resulting in carbonaceous shale beds) interrupted by storm deposition (causing deposition of graded silt/mud couplets). Alternation of carbonaceous beds with silt/mud couplets gives these shales a characteristic striped appearance. Along the basin margins a pyrite-rich sub-facies of these striped shales is found locally, consisting of laminated pyrite beds that alternate with non-pyritic silt/mud couplets. Laminated pyrite beds in pyritic striped shales are interpreted as mineralized microbial mats because of wavy-crinkly internal laminae and because of the direct association with unmineralized striped shales that contain microbial mat deposits. Excess iron in pyritic shale horizons was probably supplied by terrestrial runoff in colloidal form. Iron hydroxides, introduced by rivers into basin marginal lagoons, flocculated, and were then incorporated into microbial mats and reduced to pyrite upon burial.

Introduction

Within the Newland Formation shales of a characteristic striped appearance are common. These striped shales contain deposits of benthic microbial mats and were described earlier by Schieber (1986a). A pyrite-rich variant of these striped shales is described here. These pyritic shales occur along the margins of the Helena embayment, an eastern extension of the Mid-Proterozoic Belt basin. The sediment fill of the Helena embayment consists predominantly of rocks of the Lower Belt Supergroup (Harrison, 1972). Pyritic shales from the southern Little Belt Mountains (Fig. 1) were investigated in detail. A brief description of stratigraphy, sedimentary setting and basin evolution is given in Schieber (1986b). Pyritic shales that are similar to those of the Newland Formation have been described from Proterozoic shale sequences in Australia, and are in places found in association with stratiform base-metal mineralization (Bennet, 1965; Cotton, 1965; Mathias et al., 1973; Loudon et al., 1975).

A scheme of the stratigraphy of the Helena embayment is shown in Fig. 2. Belt sedimentation commenced with deposition of the basal Neihart Quartzite (Weed, 1899). The Neihart Quartzite grades upsection into the Chamberlain Shale (Walcott, 1899) and is in turn overlain by the Newland Formation. In the southern Little Belt Mountains the Newland Formation can be subdivided (Nelson, 1963) into a lower member (dolomitic shales) and an upper member (alternating shale and carbonate packages). A sandstone-

0037-0738/89/$03.50

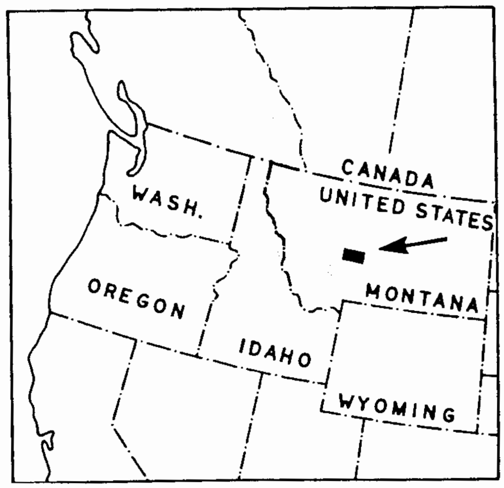

Fig. 1. Location map. Present-day outline of Belt basin indicated by stipple pattern. The Helena embayment is the eastern extension of the basin. The arrow and the blackened rectangle point out the study area in the Little Belt Mountains.

bearing unit is found in the transition between the upper and lower member of the Newland Formation, and was informally named the "Newland Transition Zone" (NTZ) by Schieber (1985). Deposition of the NTZ marks a major regression, and the Helena embayment changed from a smooth depression to an east–west-trending half-graben with active faults along the southern margin. Pyritic shales of the southern Little Belt Mountains occur mainly in the upper portion of the NTZ. Belt sediments in the Little Belt Mountains are unmetamorphosed.

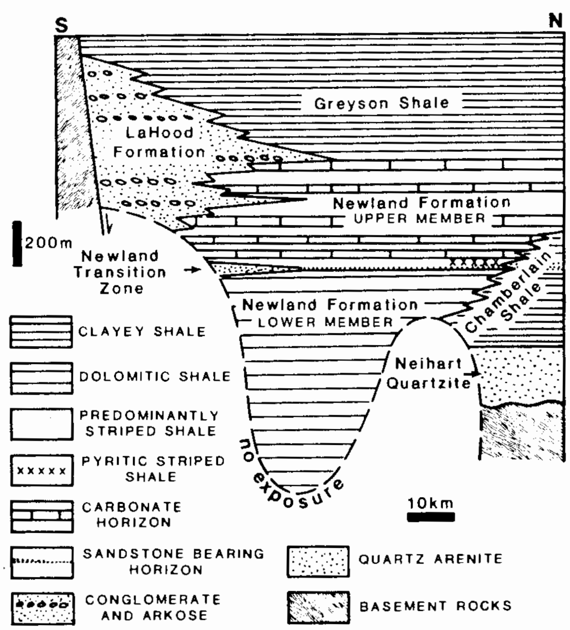

Fig. 2. Stratigraphic overview for the Helena embayment. Based on data from McMannis (1963), Boyce (1975), and Schieber (1985).

Pyrite in the Newland shales

The occurrence of pyrite

Pyrite occurs throughout the shales of the Newland Formation (lower and upper member) as tiny spherical grains or as euhedral crystals (0.001–0.01 mm in size). Spherical and euhedral forms of pyrite occur together in any given sample. These pyrite crystals are either scattered irregularly throughout the rock, or are clustered together as framboids (0.02–0.25 mm in size), or may form fine wavy-lenticular pyritic laminae (0.01–0.2 mm thick). Bundles of such laminae form laminated pyrite beds. Whereas scattered and framboidal pyrite is a common minor constituent (up to 4%) of all the shales in the Newland Formation, laminated pyrite beds are only found in distinct horizons of pyritic shale.

Laminated pyrite

Laminated pyrite beds are some millimeters to several centimeters thick, and are separated by beds of dolomitic clayey shale (Fig. 3). These intervening unmineralized beds have in many places silt at the bottom (may show cross-lamination, parallel lamination, and graded rhythmites) that grades upwards into dolomitic clayey shale. Thus, many of the dolomitic clayey shale beds are actually silt/mud couplets. Boundaries between pyritic and non-pyritic beds are always sharp (Fig. 3). The intimate intercalation of beds of different lithology gives the pyritic shales a striped appearance (Fig. 3). When viewed in detail, the laminated pyrite beds have a wavy-anastomosing texture and individual laminae have a wavy-crinkly appearance (Figs. 3 and 4). Between the pyritic laminae lenses and discontinuous laminae occur, consisting of sediment with variable composition (mixtures of clay, quartz silt, and fine crystalline dolomite, see Fig. 5). Shales that are lateral equiv-

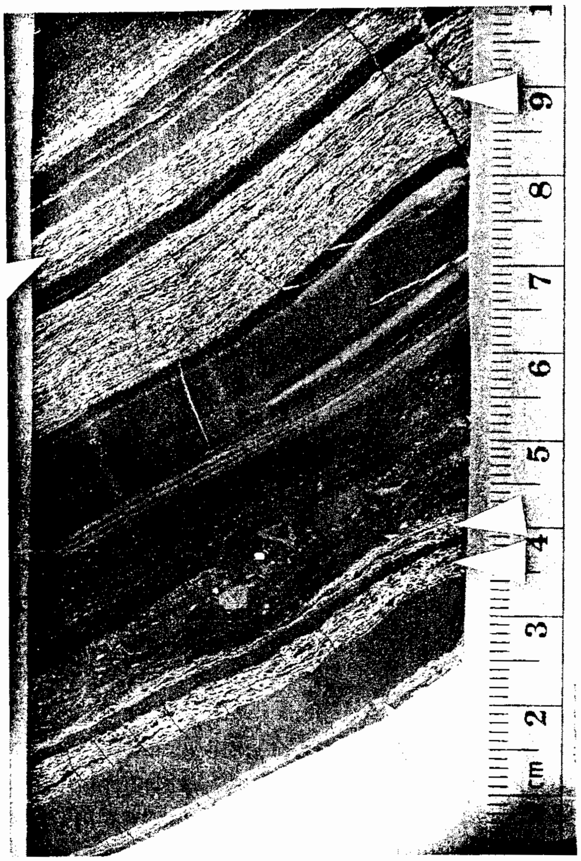

Fig. 3. Drillcore specimen of a pyritic striped shale. Laminated pyrite beds are indicated by arrows. Note the wavy-crinkly internal laminations of laminated pyrite beds, and sharp boundaries to non-pyritic interbeds. A thick storm layer with pebbles at the base and parallel laminated silt towards the top is visible in the lower half of the specimen. The scale has centimeter subdivisions.

alents of the pyritic shales have the same striped appearance; the only difference is their considerably lower pyrite content. Intervals of "normal" striped shale are also found interstratified with packages of pyritic shale, and all types of transitions between highly pyritic and "normal" striped shale were observed.

Timing of pyrite formation

In most pyrite-bearing sediments it can be shown that iron sulfides form very early in depositional history within the first few meters of burial (Berner, 1970). Dispersed and framboidal pyrite as observed in the Newland Formation forms in modern sediments very early after burial (Sweeney and Kaplan, 1973). Because in the Newland Formation grains of dispersed and framboidal pyrite are identical in appearance to pyrite grains in laminated pyrite beds (Fig. 5), it can be reasoned that pyrite in laminated pyrite beds formed very early after burial. This conclusion can be supported with textural evidence from samples of pyritic striped shale.

Evidence of the very early presence of pyrite in these sediments is for example furnished by samples which show soft-sediment deformation of laminated pyrite beds, such as convolute bedding (Fig. 6) and load casts caused by overlying conglomerate, sandstone and siltstone beds (Fig. 7). The features shown in Figs. 6 and 7 indicate that pyrite in laminated pyrite beds was present very early in the unconsolidated sediment. In some samples pyritic laminae were broken up, telescoped into each other, and pushed into underlying shale beds (Fig. 8), indicating that pyritic laminae broke up into plate-like bodies because of rigid behaviour. Such behaviour might suggest deformation and breaking of laminae after consolidation of the sediment. However, careful examination of Fig. 8 shows that, aside of the rigidly behaving and telescoped laminae (pointed out in Fig. 8), most of the pyrite bed has a homogenized/mixed appearance, and that rigidly behaving pyritic plates were pushed into underlying shale (Fig. 8). Upwelling of shale adjacent to the point where rigid pyritic plates were forced down into the shale bed (Fig. 8) indicates that the underlying sediment was still unconsolidated. On the same token, the displacement of homogenized pyritic sediment by upwelling sediment (Fig. 8) indicates that homogenized portions of the pyritic bed were equally unconsolidated. Above considerations indicate that pyritic laminae could achieve rigidity early in burial history while the remaining sediment was still unconsolidated. Reflected light microscopy of broken-up pyritic laminae shows a very high degree of pyritization and coalescing pyrite grains within these laminae. This observation suggests that "pyrite cementation" hardened individual laminae early in burial history and caused them to behave rigidly in an otherwise still unconsolidated sediment. Thus, whereas initial

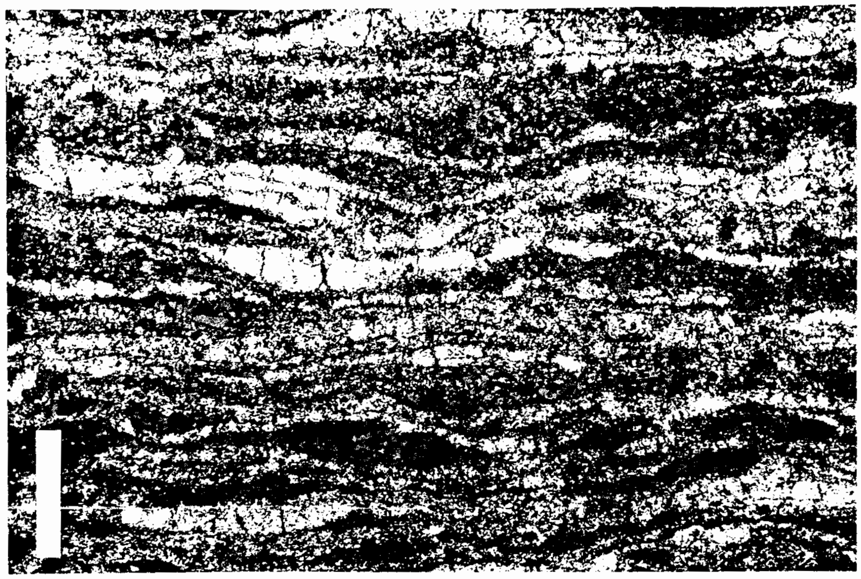

Fig. 4. Photomicrograph (reflected light) of a laminated pyrite bed. Note wavy-anastomosing internal texture and wavy-lenticular sediment intercalations between pyritic laminae. The scale bar is 0.5 mm long.

pyrite formation occurred in a completely unconsolidated sediment (Figs. 6 and 7), further burial led to "pyrite cementation" and hardening of strongly pyritic laminae in an otherwise unconsolidated sediment (Fig. 8) because of continued diagenetic pyrite growth. These fragile laminae were then broken up and telescoped in the event of soft-sediment deformation. Reworked fragments of hardened pyritic laminae and of laminated pyrite beds that are found in sandstone and conglomerate beds (Fig. 9) allow an estimate of the depth at which hardening of pyritic laminae occurred. Above sandstones and conglomerates are found as fills of erosional channels in the

Fig. 5. Photomicrograph (reflected light) of a laminated pyrite bed. It shows that individual pyritic laminae are composed of tiny pyrite crystals (white). The wavy-lenticular shale drapes between pyritic laminae consist of quartz silt, clay, and dolomite. The scale bar is 0.1 mm long.

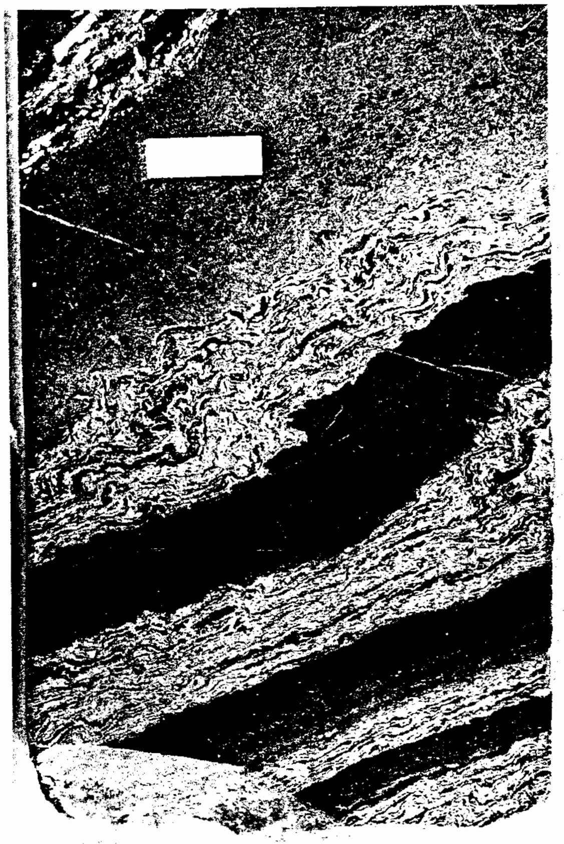

Fig. 6. Convolute bedding caused by soft sediment deformation in a sample of pyritic striped shale. Pyritic beds are light coloured. Scale bar is 10 mm long.

pyritic shale facies, and because these channels are up to 50 cm deep, pyritization and hardening of pyritic laminae must have occurred within the uppermost 50 cm of the sediment. Thus, textural evidence as well as comparison with modern sediments suggests that pyrite in pyritic striped shales of the Newland Formation formed very early in burial history.

Could the laminated pyrite beds be mineralized microbial mats?

"Normal" striped shale

A substantial portion of the Newland Formation is made up of striped shales that consist of interbedded dolomitic clayey shales and carbonaceous silty shales (Fig. 10), and these shales are the key to understand the origin of the pyritic shales described above. A detailed study of the sedimentary features of striped shales in the Newland Formation has already been published (Schieber, 1986a). From that study it appears that the carbonaceous silty shale beds in these striped shales are the result of the growth of benthic microbial mats. The main evidence for a microbial mat interpretation is summarized in the following paragraph.

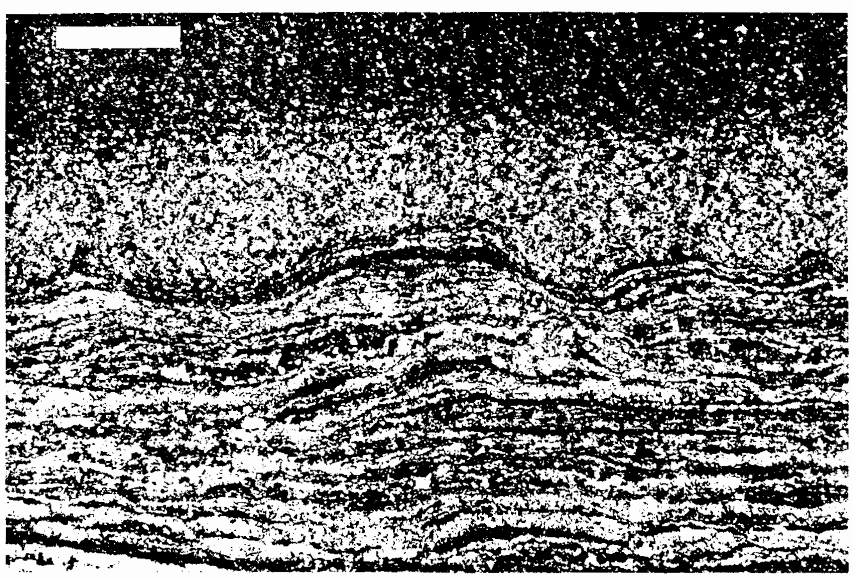

Fig. 7. Photomicrograph (reflected light) of a laminated pyrite bed that is overlain by graded silt/mud couplet. Note the load casts of silt into underlying pyritic bed. The scale bar is 0.5 mm long.

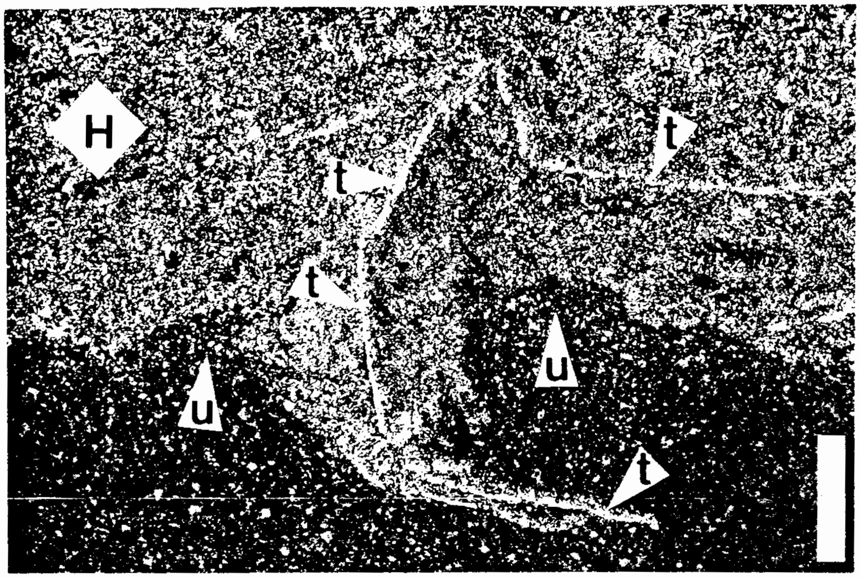

Fig. 8. Photomicrograph (reflected light) from the base of a pyritic bed that has undergone soft sediment deformation. It shows a diagenetically "pyrite cemented" and hardened pyritic lamina (arrows *t*) that was broken up into plate-like bodies during soft sediment deformation, and then telescoped and pushed into the still soft underlying shale bed. That the homogenous appearing portion of the pyritic bed (indicated as *H*) and the underlying shale were still unconsolidated when the breaking-up of the pyritic lamina occurred is indicated by upwelling of shale at locations marked with arrows *u* and the consequent displacement of homogenous pyritic sediment. Homogenized pyritic sediment is only found at the very base of this pyritic bed, and homogenization could be a consequence of soft-sediment deformation. Scale bar is 0.5 mm long.

Irregular wavy-crinkly laminae in carbonaceous silty shale beds (Fig. 11) resemble stromatolitic laminae as described by Monty (1976), Bertrand-Sarfati (1976), Horodyski et al. (1977), and Krumbein and Cohen (1974), and are quite unlike the typically parallel laminae found in carbona-

Fig. 9. Photomicrograph (reflected light) of a sandstone bed in a pyritic shale horizon. Note the elongate, rigid fragments of pyrite laminae (white colour) between the sand grains. The scale bar is 0.25 mm long.

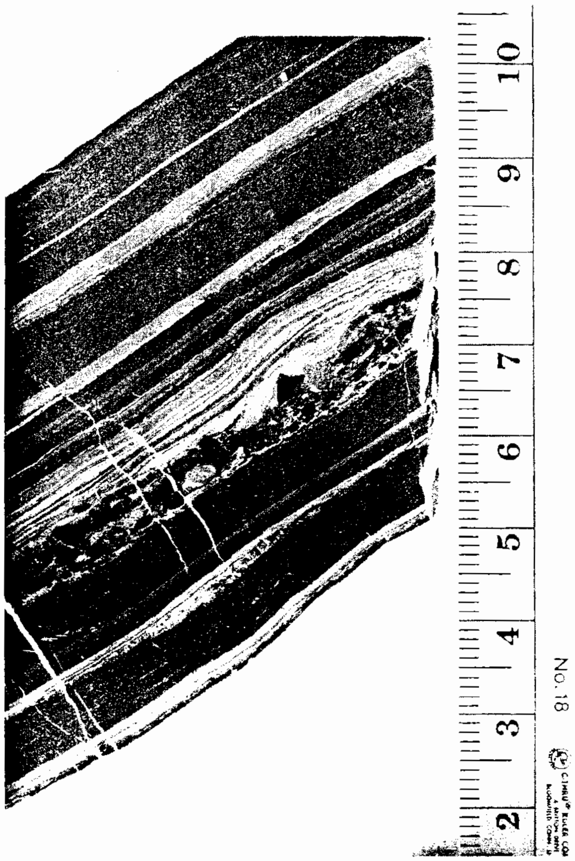

Fig. 10. Drillcore specimen of striped shale from the Newland Formation. Carbonaceous silty shale beds (microbial mat deposits) are dark gray. Note the clast/silt/mud triplet in the lower half of the specimen. Compare to the storm layer in Fig. 3. The scale has centimeter divisions.

ceous shales that accumulated in stagnant basins. The observation that carbonaceous silty shale beds behaved like a tough leathery membrane during soft-sediment deformation (Schieber, 1986a), rather than like a soupy organic muck, further supports a microbial mat interpretation of these carbonaceous beds. Rolling-up and folding over of ripped-up fragments of carbonaceous silty shale beds reveals considerable cohesive strength during transport and deposition and is further indication of a microbial mat origin (Schieber, 1986a). Remnants of filamentous bacteria and cyanobacteria that were identified in these fragments (Horodyski, 1980) further support a microbial mat interpretation.

The beds of dolomitic clayey shale were interpreted as storm deposits. Silt layers that are commonly found at the base of these shale beds show a variety of sedimentary structures, such as cross-lamination, normal grading, and graded rhythmites (in the transition to the overlying shale). These silt/mud couplets show great similarity to modern storm deposits described from the North Sea (Gadow and Reineck, 1969) and other modern shelf seas (Allen, 1965; Reineck and Singh, 1972). The occurrence of hummocky cross-stratified sandstone beds within striped shales also suggests that storms played a role in the deposition of these shales. Recurring deposition of storm layers on benthic microbial mats was responsible for the intimate interlayering of carbonaceous silty shales and dolomitic clayey shales and for the striped appearance (Fig. 10) of this type of shale facies (Schieber, 1986a).

Pyritic striped shale

Specimens of pyritic striped shale and "normal" striped shale are strikingly similar (Figs. 3, 10; cf. Schieber, 1986a, p. 522), suggesting that they are of related origin. Additional observations that indicate a common origin are:

(1) Beds of dolomitic clayey shale with silt at the bottom (silt/mud couplets) occur in "normal" as well as in pyritic striped shales (Figs. 7, 11, and 12, and Schieber, 1986a, p. 526), and have the same sedimentary structures in the silt portion (cross-lamination, parallel lamination, graded rhythmites). Sedimentary structures were observed in polished slabs and in thin section.

(2) Laminated pyrite beds (in pyritic striped shale) and carbonaceous silty shale beds (in "normal" striped shale) have the same wavy-anastomosing internal texture and the same wavy-crinkly appearance of individual laminae (Figs. 4, 11, 12 and 13).

(3) Sediment between individual pyritic laminae consists of lenses and discontinuous laminae of a mixture of clay, dolomite, and quartz silt (Fig. 5), and is in every respect identical to shale drapes and silt-rich lenses that occur between carbonaceous silty laminae in carbonaceous silty shale beds (Fig. 13) of "normal" striped shale.

(4) "Normal" striped shales are the lateral equivalents of pyritic striped shales, and are also interbedded with pyritic striped shales.

Fig. 11. Irregular carbonaceous laminae in carbonaceous silty shale beds. These laminae are considered to be of microbial origin. A thin silt/mud couplet is indicated by the arrow in the upper half of the photo. The arrow points to the boundary between the silt and the mud portion of the couplet. The scale bar is 0.5 mm long.

(5) A smooth transition in pyrite content can be observed, from "normal" carbonaceous silty shale beds with 1–4 vol.% pyrite (Fig. 14), over beds with intermediate amounts of pyrite (Fig. 12), to highly pyritic laminated pyrite beds with as much as 50 vol.% pyrite (Fig. 4).

Two conclusions can be drawn from these observations and textural comparisons: (1) carbona-

Fig. 12. Photomicrograph of a sample of pyritic striped shale. The photo was taken under a combination of reflected and transmitted light. A laminated pyrite bed that consists of approximately 25% pyrite makes up the lower half of the photo. Several pyritic laminae in that bed are pointed out with arrows, and pyrite grains in these laminae show up as fine white dots. Compare the irregular crinkly laminae in the laminated pyrite bed with those in the carbonaceous silty shale bed shown in Fig. 11. A thin silt/mud couplet is pointed out by arrow *m* (points at boundary between silt and mud). The scale bar is 0.25 mm long.

Fig. 13. Photomicrograph (transmitted light) of carbonaceous silty shale in striped shales from the Newland Formation. Note the three textural components: (1) drapes of dolomitic clayey shale (arrow *d*); (2) carbonaceous silty laminae (arrow *c*); and (3) tiny silt-rich lenses (arrow *s*). Scale bar is 0.1 mm long.

ceous silty laminae in carbonaceous silty shale beds (in "normal" striped shale) are the direct equivalents of pyritic laminae in laminated pyrite beds (pyritic striped shale); (2) pyritic striped shales are simply a pyrite-rich variety of the striped shales that are so common in the Newland Formation. The first conclusion is also supported by the observation that in "normal" striped shales most of the pyrite is found in the carbonaceous silty laminae of carbonaceous silty shale beds (Fig. 14). Finally, under the assumption that carbonaceous silty shale beds in "normal" striped shales are fossil microbial mats (Schieber, 1986a), the textural equivalency between pyritic and "normal" striped shales leads to the conclusion that laminated pyrite beds in pyritic striped shales are pyrite-mineralized benthic microbial mats.

Origin of pyritic shale horizons

Pyritic shale horizons in the southern Little Belt Mountains extend laterally for as much as 8 km, may reach up to 60 m thickness, can contain on the order of 10^8 tons of iron in pyrite (Schieber, 1987a), and grade laterally into "normal" striped shales. Even though laminated pyrite beds contain up to 50% pyrite by volume, averaging over the whole thickness of a pyritic shale horizon results in an average iron content of about 10% (calculated as metallic iron). Of this iron, 75% are contained in pyrite and the remaining 25% in the terrigenous clastic component. Thus, even though the amount of iron in individual pyritic shale horizons is of the same magnitude as found in Phanerozoic ironstone deposits (Schieber, 1987a), the pyritic shales have no economic significance.

The possible source of the iron that accumulated in these pyritic shale horizons was discussed in detail by Schieber (1987a), and a summary of pertinent conclusions follows below. Because of the reducing character of the sediments below the pyritic shale horizons, it is considered quite unlikely that iron was mobilized from within the basin. An alternative model in which iron is brought into the basin by continental runoff is clearly feasible (Schieber, 1985, 1987a) and in accord with the sedimentary history of the basin. Only very small amounts of iron are needed in the terrestrial runoff to account for the iron in the pyritic shale horizons. Considering the oxidation state of the Mid-Proterozoic atmosphere (Schidlowski et al., 1975), iron was probably introduced into the basin in the form of iron oxyhydroxides.

"Normal" striped shales in the Newland For-

Fig. 14. Photomicrograph (combined reflected and transmitted light) of carbonaceous silty shale bed in "normal" striped shale. Pyrite (tiny white specks) occurs mainly in the carbonaceous silty laminae. Arrows *1*, *2*, and *3* point out larger, spherical pyrite grains, the other arrows point out areas with abundant small pyrite grains. Scale bar is 0.1 mm long.

mation were deposited subaqueously within reach of storm waves (Schieber, 1986a, 1987b). In pyritic shale horizons interbedded sandstones contain abundant erosion surfaces, erosive channels, cross-bedding, and variable amounts of intraclasts. These features indicate episodic strong currents, high-energy events (such as storms), and fairly shallow-water conditions during deposition of pyritic striped shales. Stratigraphic and sedimentologic investigations by Schieber (1985) led to the conclusion that pyritic striped shales accumulated in coastal embayments that were partially enclosed by offshore sandbars.

Pyrite-rich shales are usually thought to accumulate in quiet water under anoxic conditions, but such a notion is contradicted by the high-energy sedimentary features in the interbedded sandstones in the case of the pyritic shales of the Newland Formation. However, in the Proterozoic strongly reducing shales may have accumulated in shallow aerated environments in the presence of benthic microbial mats (Schieber, 1986a). Microbial mats act as an ecological membrane that causes several environmental parameters, such as Eh, H_2S concentration, dissolved O_2, and light intensity, to undergo abrupt changes at the interface (Bauld, 1981). Below such a mat strongly reducing conditions can exist despite aerated water above the mat (Bauld et al., 1980). Similar to their modern counterparts, benthic microbial mats in nearshore lagoons of the Newland Formation were probably sticky and gelatinous (Golubic, 1976). Iron hydroxides that flocculated in nearshore areas would eventually become trapped on the mat surface, and would be transformed into pyrite after incorporation into the buried reducing layers

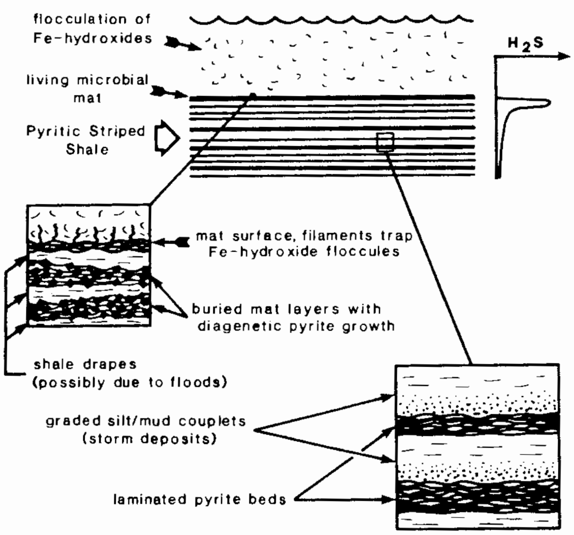

Fig. 15. Proposed formation of pyritic striped shales. Fe-hydroxide flocculates are trapped by microbial mat filaments and converted to pyrite after burial because of large sulfate reduction rates below the mat surface. Enlarged portion to the left (box is approximately 0.5 mm high) shows trapping of Fe-hydroxides and alternation of Fe-rich (pyritic) mat layers with shale drapes (consisting of clay, dolomite, and quartz silt, see also Figs. 4 and 5). The latter may be related to pulses of sediment that were supplied to nearshore areas during river floods (Schieber, 1986a). Deposition of silt/mud couplets by storms interrupted microbial mat growth (enlarged portion to the right, box is approximately 5 cm high), and new mats were established on top of storm deposits (see also Figs. 3 and 8).

of the mat. The envisioned scenario for formation of pyritic striped shales is summarized in Fig. 15.

Conclusion

The pyritic striped shales in the Newland Formation are a pyrite-rich variant of the "normal" striped shales described earlier (Schieber, 1986a). Pyrite-rich shale beds are mineralized benthic microbial mats that accumulated in nearshore lagoons. Intercalated storm deposits (silt/mud couplets) give this type of shale its characteristic striped appearance. Iron was probably supplied to these shales by riverine colloidal iron oxyhydroxides that flocculated in nearshore areas and then was trapped on microbial mat surfaces. Upon burial, pyrite formation commenced in the reducing environment below the mat. Improved understanding of this type of pyritic shales could be of economic importance because similar appearing Proterozoic shales elsewhere are associated with stratiform base-metal deposits.

Acknowledgements

Research on pyritic shales of the Newland Formation was supported by Anaconda Minerals Co. Discussions with Drs. R.W. Castenholz and G.J. Retallack were instrumental in shaping my ideas about microbial mat growth and potential mineralization.

References

Allen, J.R.L., 1965. Late Quaternary Niger delta and adjacent areas: sedimentary environments and lithofacies. Bull. Am. Assoc. Pet. Geol., 49: 547–600.

Bauld, J., 1981. Geobiological role of cyanobacterial mats in sedimentary environments: production and preservation of organic matter. BMR J. Aust. Geol. Geophys., 6: 307–317.

Bauld, J., Johns, I.A., Plumb, L.A., Reed, M.R. and Skyring, G.W., 1980. Sulphate reduction in algal mat sediments. Baas Becking Geobiol. Lab. Annu. Rep. 1980, pp. 21–25.

Bennet, E.M., 1965. Lead-zinc-silver and copper deposits of Mount Isa. In: J. McAdrew (Editor), Geology of Australian Ore Deposits. 8th Commonw. Min. Metall. Congr., Melbourne, 1: 1233–1246.

Berner, R., 1970. Sedimentary pyrite formation. Am. J. Sci., 268: 1–23.

Bertrand-Sarfati, J., 1976. An attempt to classify Late Precambrian stromatolite microstructures. In: M.R. Walter (Editor), Stromatolites, Developments in Sedimentology, 20. Elsevier, Amsterdam, pp. 251–259

Boyce, R.L., 1975. Depositional systems in the LaHood Formation (Belt Supergroup), southwestern Montana. Ph.D. Dissertation, University of Texas, Austin, Texas, 247 pp.

Cotton, R.E., 1965. H.Y.C. lead-zinc-silver deposit, McArthur River. In: J. McAdrew (Editor), Geology of Australian Ore Deposits. 8th Commonw. Min. Metall. Congr., Melbourne, 1: 197–200.

Gadow, S. and Reineck, H.E., 1969. Ablandiger Sandtransport bei Sturmfluten. Senckenbergiana Marit., 1: 63–78.

Golubic, S., 1976. Organisms that build stromatolites. In: M.R. Walter (Editor), Stromatolites. Elsevier, New York, N.Y., pp. 113–126.

Harrison, J.E., 1972. Precambrian Belt basin of northwestern United States: its geometry, sedimentation, and copper occurrences. Geol. Soc. Am., Bull., 83: 1215–1240.

Horodyski, R.J., 1980. Middle Proterozoic shale facies microbiota from the lower Belt Supergroup, Little Belt Mountains, Montana. J. Paleontol., 54: 649–663.

Horodyski, R.J., Bloeser, B. and Von Der Haar, S., 1977. Laminated algal mats from a coastal lagoon, Laguna Mormona, Baja California, Mexico. J. Sediment. Petrol., 47: 680–696.

Krumbein, W.E. and Cohen, Y., 1974. Biogene, klastische und evaporitische Sedimentation in einem mesothermen monomiktischen ufernahen See (Golf von Aquaba). Geol. Rundsch., 63: 1035–1065.

Loudon, A.G., Lee, M.K., Dowling, J.F. and Bourn, R., 1975. Lady Loretta silver-lead-zinc deposit. In: C.L. Knight (Editor), Economic Geology of Australia and Papua New Guinea, I. Metals. Australas. Inst. Min. Metall. Monogr., 5: 66–74.

Mathias, B.V., Clark, G.J., Morris, D. and Russel, R.E., 1973. The Hilton deposit—stratiform silver-lead-zinc mineralization of the Mt. Isa type. BMR Geol. Geophys. Bull., 141: 33–58.

McMannis, W.H., 1963. LaHood Formation—a coarse clastic facies of the Belt Series in southwestern Montana. Geol. Soc. Am., Bull., 74: 407–436.

Monty, C.L.V., 1976. The origin and development of cryptalgal fabrics. In: M.R. Walter (Editor), Stromatolites, Developments in Sedimentology 20. Elsevier, Amsterdam, pp. 193–249.

Nelson, W.H., 1963. Geology of the Duck Creek Pass quadrangle. U.S. Geol. Surv., Bull., 1121J, 56 pp.

Reineck, H.E. and Singh, I.B., 1972. Genesis of laminated sand and graded rhythmites in storm-sand layers of shelf mud. Sedimentology, 18: 123–128.

Schidlowski, M., Eichmann, R. and Junge, C.E., 1975. Precambrian sedimentary carbonates: carbon and oxygen isotope geochemistry and implications for the terrestrial oxygen budget. Precambrian Res., 2: 1–69.

Schieber, J., 1985. The relationship between basin evolution and genesis of stratiform sulfide horizons in Mid-Proterozoic sediments of central Montana (Belt Supergroup). Ph.D. Dissertation, University of Oregon, Eugene, Oreg., 811 pp.

Schieber, J., 1986a. The possible role of benthic microbial mats during the formation of carbonaceous shales in shallow Mid-Proterozoic basins. Sedimentology, 33: 521-536.

Schieber, J., 1986b. Stratigraphic control of rare-earth pattern types in Mid-Proterozoic sediments of the Belt Supergroup, Montana, U.S.A.: implications for basin analysis. Chem. Geol., 54: 135-148.

Schieber, J., 1987a. Small scale sedimentary iron deposits in a Mid-Proterozoic basin: viability of iron supply by rivers. In: P.W.U. Appel and G. LaBerge (Editors), Precambrian Iron-Formations. Theophrastus Publications, Athens, pp. 267-295.

Schieber, J., 1987b. Storm dominated epicontinental clastic sedimentation in the Mid-Proterozoic Newland Formation, Montana, U.S.A.. Neues Jarhb. Geol. Paläontol., Monatsh., 27: 417-439.

Sweeney, R.E. and Kaplan, I.R., 1973. Pyrite formation: laboratory synthesis and marine sediments. Econ. Geol., 68: 618-634.

Walcott, C.D., 1899. Precambrian fossiliferous formations. Geol. Soc. Am., Bull, 10: 199-244.

Weed, W.H., 1899. Descriptions of the Little Belt Mountains quadrangle (Montana). U.S. Geol. Surv., Geol. Atlas Folio 56.